Egypt. J. Chem. **Vol. 65,** No. 2 pp. 439 - 448 (2022)

Egyptian Journal of Chemistry

http://ejchem.journals.ekb.eg/

Synthesis, Characterization, Crystal structure of 4-(4-Bromo-phenyl)-2,6-dimethyl-1,4-dihydro-pyridine-3,5-dicarboxylic acid diethyl ester: Hirshfeld surface analysis and DFT calculations

D. Parthasarathi[a], M. Syed Ali Padusha[a*], S. Suganya[b], P. Kumaradhas[b], Ayyiliath M. Sajith[c], Muthipeedika Nibin Joy[d]

[a]*Post Graduate and Research Department of Chemistry, Jamal Mohamed College, Bharathidasan University, Tiruchirappalli, Tamilnadu,620 020, India*

[b]*Laboratory of X-Ray Crystallography and Computational Molecular biology, Department of Physics, Periyar University, Salem-636 01, India*

[e]*Ortin laboratories Pvt.Ltd, Malkapur Village, Choutuppal Mandal, Hyderabad, Telengana-508252, India*

[d] *Innovation center for Chemical and Pharmaceutical Technologies, Institute of Chemical Technology, Ural Federal University, 19Mira Street, Yekaterinburg, Russia-620002*

Abstract

The title compound dihydro-pyridine was synthesized and structure is established by FT-IR, ^{1}H NMR, and ^{13}C NMR spectral analysis. The SC-XRD analysis has been carried out for the determination of molecular structure and its disclosed that crystal relates to monoclinic crystal phase, P21/n1 space group and cell parameters are a= 10.2314(2), b = 7.5215(1), c = 24.5475(4), α = 90, β = 97.921(1)° γ = 90 with 0.34 x 0.33 x 0.30 crystal size. The crystal lattice exhibits inter-molecular H-bonding between N1—H1A—O1. Further inter contacts of the crystal lattice were determined by 3-D Hirshfeld surface (HSA) as well as percentage of contributions have been computed through 2D finger plot depiction. Moreover, bond length, bond angle and torsion angles have been correlated to respective output results of B3LYP/6-311++G(d,p). The electrophilic and nucleophilic characters have been studied through molecular electrostatic potential (MEP) analysis.

Keywords: 1,4 Dihydro pyridine, SC-XRD, N-H-O interaction, Hirshfeld surfaces, DFT analysis

1. Introduction

Heterocyclic chemistry has gained great attention of researchers across the globe in recent decades. The heterocyclic compounds play an important function vital role in the field of pharmaceutical and industrial chemistry [2]. Among the several heterocyclic compounds, 1,4 dihydropyridine derivatives has emerged significant class of heterocycles. The 1,4 dihydropyridine derivatives was reported by Arthur Hantzch in 1881[3]. These derivatives are extensively utilized as calcium channel antagonist [4-6]. Apart from the use of cardiovascular agents, these derivatives possess various pharmacological properties [7-16]. These biological aspects of this medicinally relevant core demand for the development of novel methodologies that allow diversity around this framework. Among the several synthetic protocols employed, one-pot multicomponent reactions are the perhaps the most successful method for synthesizing 1,4 dihydropyridine (1,4 DHP) derivatives [17-19].

Moreover, the quantum mechanical calculation plays a vital role for describing the structural elucidation, electronic and chemical behaviour of the molecule. Additionally the intermolecular interactions analysis provides a detailed intermolecular interaction of the crystal lattice [20,21]. The crystal structure of substituted 1,4 dihydropyridine derivatives were reported by various researchers [22]. Boulcina et al have reported the crystal structure of bromo substituted 1,4 dihydropyridine derivative. The synthetic methodology involves the condensation

*Corresponding author e-mail: sp@jmc.edu.; (Dr. M. SYED ALI PADUSHA).
Receive Date: 02 August 2021, Revise Date: 16 August 2021, Accept Date: 24 August 2021
DOI: 10.21608/EJCHEM.2021.88473.4256

reaction of aromatic aldehyde, ethyl acetoacetate and aqueous ammonia/urea in ethanol. However, a detailed study of the compound, including the Hirshfeld surface analysis and DFT calculations are still unexplored [23,24]. We herein report the molecular structure investigation by theoretical and experimental methods. The synthetic methodology involves ethyl acetoacetate aromatic aldehyde and ammonium acetate under milder reaction condition. To our delight, we obtained the expected title compound in 98% yield after crystallization.

In our previous work describes the synthesis, crystal structure and DFT analysis of 4-(4-4-fluro-phenyl)-2,6-dimethyl-1,4-dihydro-pyridine-3,5-dicarboxylic acid diethyl ester [25]. The present work, we report the molecular structure investigation of 4-(4-Bromo-phenyl)-2,6-dimethyl-1,4-dihydro-pyridine-3,5-dicarboxylic acid diethyl ester. The spectral analysis like FT-IR ,^{1}H NMR and ^{13}C NMR analysis reveal that the nature functional frequencies, proton environment and carbon nature in the structure. The single crystal X-RD analysis proved the molecular arrangement as well as nature of hydrogen bonding present in the crystal. The intermolecular interactions of the compound were determined by Hirshfeld surface analysis. Moreover, the geometric parameters are in good correlation with the crystallographic parameters.

2. Experimental

All chemicals and reagents have been obtained from Sigma Aldrich and were used without purging. The thin layer chromatography was carried out with the assistance of silica gel (Mesh120) with glass plates. The buchi apparatus has been used to check the melting point. The FT-IR spectrum has been detected on Bruker Alpha II spectrophotometer. The ^{1}H-NMR and ^{13}C-NMR spectra were detected on Bruker (400 MHz) high-performance FT-NMR spectrometer. The chemical shift (δ) and coupling constants (J) were measured by ppm and Hz respectively. The CHN analysis was carried out using Elementar varioMICRO select analyzer.

2.1. Synthetic procedure

A mixture of 4-bromo benzaldehyde (0.01M), ethyl acetoacetate (0.02 M) and ammonium acetate (0.015 M) were dissolved in 30 mL ethanol + water (60+40%). The reaction mixture was stirred for 2 h at RT. The progress of the reaction was monitored by TLC. After completion of the reaction, the mixture was poured into crushed ice; solid was filtered, dried and recrystallized from ethanol.

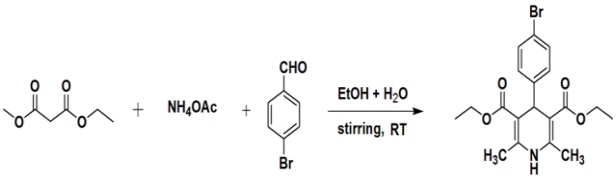

Scheme 1. Synthesis of crystalized molecule

Yellow color solid; yield: 98%; m.p. 184-186; IR: 3355 cm^{-1} (N-H), 2987 cm^{-1} (Ar-CH), 2958 cm^{-1} (R-CH), 1693 cm^{-1} (C=O), 1649 cm^{-1} (C=C), 580 cm^{-1} (C-Br); ^{1}H NMR (400 MHz, $CDCl_3$) δ 7.21-.24 (dd, J = 7.9, 5.2 Hz, 2H, Ar-H), 6.87 (qt, J = 5.5, 2.4 Hz, 2H Ar-H), 6.20 N-H), 4.96 (s, 1H), 4.12 – 4.06 (m, 4H, CH2), 2.28-2.30 (dd, J = 11.2, 6.2, 2.6 Hz, 6H, -OCH3), 1.19-1.23 (dt, J = 7.1, 3.6 Hz, 6H, -CH_3). ^{13}C NMR (101 MHz, $CDCl_3$) δ 167.74, 167.55, 162.55, 160.13, 144.29, 143.82, 130.89, 129.45, 129.38, 114.60, 114.39, 104.16, 103.79, 59.81, 39.32, 39.04, 19.60, 19.31, 14.26. Anal Calc. for $C_{19}H_{22}BrNO_4$; C, 55.89; H, 5.43; Br, 19.57; N, 3.43; O, 15.67. Found; C, 55.79; H, 5.31; Br, 19.48; N, 3.32; O, 15.63. GC-MS (m/z): 408.

2.2 XRD determination and computational details

The crystallographic data of the compound were collected at room temperature (293 K) on a Bruker D8 Quest ECO diffractometer using MoKα radiation (0.71073 Å) and the APEX-III program was used to monitor the data collection [26]. The cell refinement and data reduction was detected through Bruker SAINT Software package. The absorption effect data were corrected using the numerical method (SADABS) and refined using SHELXS-2014 & SHELXL-2014 programmers [27-29]. The monoclinic crystal system yielded 43084 reflections. The non-hydrogen atoms were resolved anisotropically and hydrogen atoms were refined geometrically [C-H= 0.96 A] using riding model Uiso(H) =1.5 Ueq(C). Uiso= 1.5 (Cmethyl). The crystal packing and geometrical parameters were accomplished using MERCURY and ORTEP [30,31]. The quantum chemical calculations were computed by DFT-Gaussian 09 version by B3LYP/6-311++G(d,p)

method. The Gauss view 5.0 programs was used to interpret the data and structural visualization of the compound [32,333]. The corresponded 2-D finger prints and Hirshfeld surface was accomplished through crystal explorer 3.0. [34].

3. Results and Discussions

3.1. FT-IR, ^{1}H and ^{13}C NMR analysis

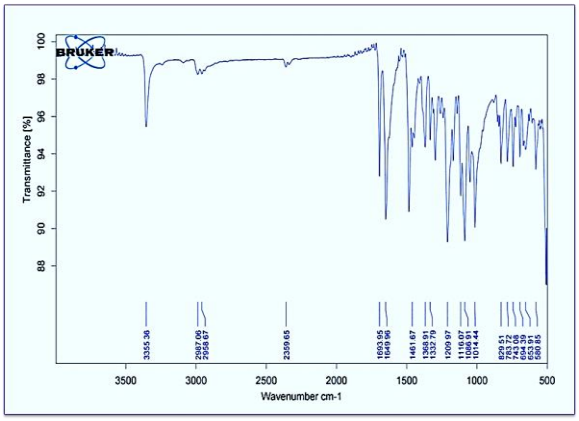

Fig.1 FT-IR spectrum of the molecule

Fig.1. describes the N-H peak appeared at 3355 cm^{-1}. The existence of a band at 2987 cm^{-1} is ensured for aromatic C-H band. A peak observed at 1693 cm^{-1} is assigned to C=O band. A band appeared at 1649 cm^{-1} is corresponding to C=O group. A peak observed at 580 cm^{-1} is confirms the C-Br stretching [35]. The ^{1}H NMR spectrum describes the aromatic protons are observed at δ 7.21-.6.87 ppm. A singlet observed from δ 4.96 ppm is attributed to -CH proton. A multiplet observed at δ 4.12 – 4.06 ppm The existence of a singlet at δ 6.20 ppm is attributed to NH proton. The methyl group in the pyridine ring is observed by a doublet of triplet observed at δ 1.23-1.19 ppm. A doublet of doublet peak observed at δ 2.32-2.28 ppm is assigned to CH_3 proton. The ^{13}C NMR spectrum describes the signal appeared at δ 167.73 and 167.55ppm confirms the presence of C=O. A multiplet signal appeared in the region δ 144.29 -114.39 ppm is assigned to aromatic carbon. A peak appeared at δ 59.81ppm is assigned to O-CH_3 carbon. A signal observed at δ 39.32 ppm is corresponding to benzylidine CH carbon. The presence of methyl carbon at pyridine ring is ensured by the appearance of a peak at δ 19.60 and 19.31. A peak appeared at δ 14.26 ppm is attributed to methylene carbon. The ^{1}H and ^{13}C NMR data are given in **Fig. 2** and **Fig. 3** [36,37].

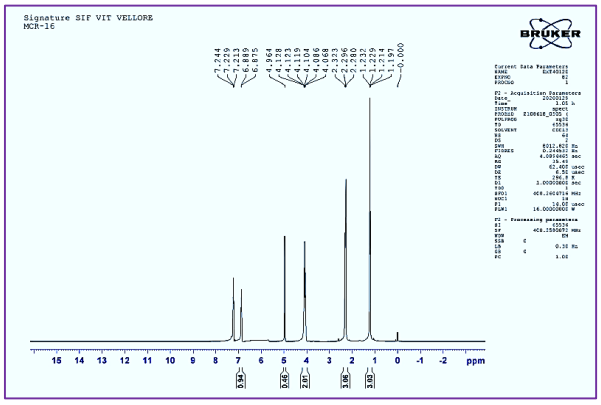

Fig.2. ^{1}H NMR spectrum of the molecule

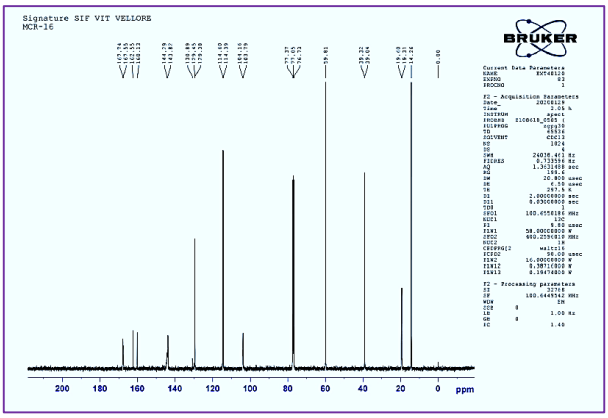

Fig.3. ^{13}C NMR spectrum of the molecule

3.2. Single crystal XRD description

The SC-XRD analysis report of the compound has been deposited in Cambridge Crystallographic Data Centre with CCDC Number: **2040812** and this data can be freely collected by request form the www.ccdc.cam.ac.uk/data_request/cif online server.

The title compound (C_{19} H_{22} Br NO_4) was recrystallized using ethanol solvent by slow evaporation method. The crystal lattice shows monoclinic crystal phase, $P21/n_1$ space group and cell parameters a=10.2314(2), b=7.5215(1), c =24.5475(4), β=97.921(1)°, Z= 4, and V=1871.04(5) $Å^3$, Crystal size is 0.34 x 0.33 x 0.30 mm and Goodness of fit on F2 =1.05. The refinement details and crystal structure information are provided in **Table 1** and ORTEP representation is displayed in **Fig. 4 .** In 1,4 dihydro pyridine ring was characterized by flattened boat conformation, N1 and C7 atoms are arranged from the base of the boat plane, which is confirmed by N1/C8/C9/C10/C11 atoms. The presence of N—H1A bond is ensured by bond length = 0.84 (2). The bond angle for C10—N1—H1A =116 (2)° and C9—N1—

H1A = 120 (2)°. Torsion angles are another structural description of the crystallized compound. The aromatic ring connected with 1,4 dihydropyridine ring which ensured by torsion angle found to be C2—C3—C7—C11=57.8 (3)° and C2—C3—C7—C8 =-65.8 (3)°. The torsion angles for 1,4 dihydro pyridine ring is found to be C12—C11—C10—N1 = 174.4 (2)º and C17—C8—C9—N1 = -178.7 (2)º [38,39]. The two ethoxy groups are ensured by the torsion angles found to be C7—O2—C16—C8 = 176.01 (16)º and C13—O3—C12—C1 = -174.76 (15)º. The torsion angles for 4-bromo phenyl ring is found to be Br1—C6—C5—C4 = -180.0 (2)°. The selected bond length bond angles and torsion angles are tabulated in Table 2 and Table 3 respectively. The flattened boat structure was confirmed from the displacement (Å2) values found for N1= 0.0597 (13)Å2 and C7= 0.0504 (12)Å2 [40,41]. The compound exhibits inter-molecular H-bonding between N1—H1A-----O3 with the bond distance of 3.045(3)A°. The H-bonding interaction and with bond distance are displayed in **Table.4** and **Fig.5** respectively.

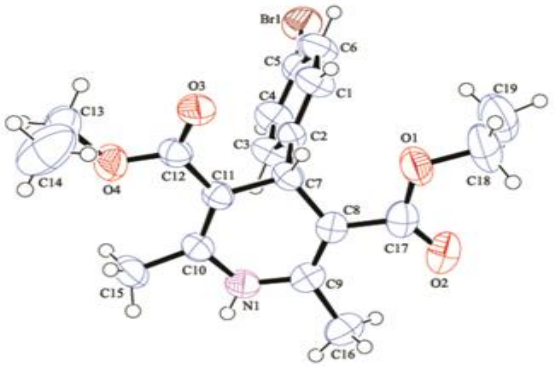

Fig. 4. ORTEP plot of the molecule with 50% probability and atom labelling

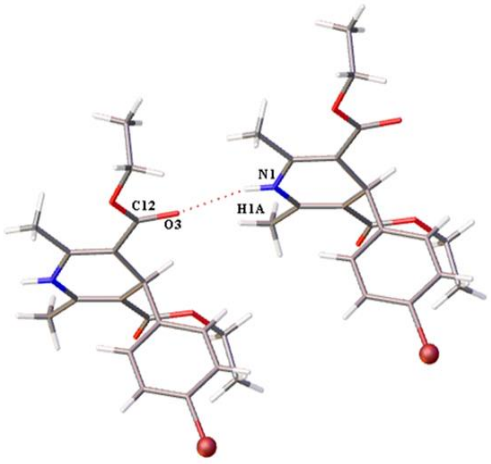

Fig.5. *N-H-O interaction of the molecule*

Table 1. Crystal data and structure refinement details.

CCDC Number	**2040812**
Chemical formula	$C_{19}H_{22}BrNO_4$
Molecular weight	408.29 g/mol
Crystal system,	Monoclinic &
Space group	$P2_1/n_1$
Temperature (K)	293
Unit cell dimensions (Å)	a =10.2314(2) b = 7.5215(1) c = 24.5475(4)
α,β,γ (˚)	α = 90 β = 97.921(1) γ = 90
V(Å^3)	1871.04(5)
Z	4
Radiation type	Mo Kα
μ (mm^{-1})	0.222
Crystal size(mm)	0.34 x 0.33 x 0.30
Limiting indices	-13<=h<=13, -10<=k<=9, -32<=l<=30
Reflections collected	4632
Independent reflections	43084 [R(int) = 0.0345]
Structure solution program	SHELXT 2014/5 (Sheldrick, 2014)
Diffractometer	Bruker D8 QUEST ECO
Refinement method	Full-matrix least-squares on F^2
Absorption correction	Numerical
T_{min}, T_{max}	0.516,0.553
Data / restraints / parameters	4632 / 0 / 234
Goodness-of-fit on F^2	1.055
Final R indices [I> σ (I	R1 = 0.0434,
All data	wR2 = 0.1257 R1 = 0.0607, wR2 = 0.1381
Largest diff. peak and hole (eÅ^{-3})	0.750 and -0.702
R.M.S. deviation from mean (eÅ^{-3})	0.056
H-atom treatment	H atoms treated by a mixture of independent and constrained refinement

Table 2. *The selected bond length (Å) and bond angle (°)*

Bond	Length(Å)	Bond	Length(Å)	Bond	Angle (°)	Bond	Angle (°)
N1—H1A	0.85 (3)	O4—C12	1.342 (3)	C8—C7—C11	110.82 (19)	C10—C11—C7	120.9 (2)
N1—C9	1.377 (3)	O4—C13	1.449 (3)	C9—N1—C10	123.6 (2)	C9—C8—C7	120.9 (2)
N1—C10	1.381 (3)	O2—C17	1.207 (3)	C9—N1—H1A	120 (2)	C2—C3—C7	121.0 (2)
C11—C7	1.526 (3)	Br1—C6	1.901 (3)	C10—N1—H1A	116 (2)	C12—O4—C13	118.2 (2)
C8—C7	1.521 (3)	C3—C7	1.523 (3)	C10—C11—C12	124.5 (2)	C17—O1—C18	117.8 (3)
O1—C17	1.347 (3)	C9—C16	1.500 (3)	C9—C8—C17	120.9 (2)	O3—C12—C11	123.2 (2)
O1—C18	1.454 (3)	C10–C15	1.500 (3)	C17—C8—C7	118.0 (2)	C1—C6—Br1	120.0 (2)

Table 3. The selected torsion angle (°)

Bond	Angle (°)	Bond	Angle (°)
C12—C11—C10—N1	174.4 (2)	C17—C8—C9—N1	-178.7 (2)
C7—C11—C10—N1	-6.2 (3)	C7—C8—C9—N1	6.0 (3)
C12—C11—C10—C15	-4.0 (4)	C17—C8—C9—C16	-0.6 (4)
C7—C11—C10—C15	175.3 (2)	C7—C8—C9—C16	-175.8 (2)
C10—N1—C9—C8	13.6 (4)	C9—N1—C10—C11	-13.4 (4)
C9—N1—C10—C15	165.3 (2)	C10—N1—C9—C16	-164.9 (2)
C17—C8—C7—C11	162.4 (2)	C12—C11—C7—C8	-158.2 (2)
C2—C3—C7—C11	57.8 (3)	C2—C3—C7—C8	-65.8 (3)
C7—C11—C12—O3	15.2 (4)	C7—C11—C12—O3	171.9 (3)
C10—C11—C12—O4	16.3 (4)	C7—C11—C12—O3	177.2 (2)
Br1—C6—C1—C2	-179.8 (2)	Br1—C6—C5—C4	-180.0 (2)

Table 4 H- Bond geometry *(Å,°)* (Symmetry codes: (i) x,-1+y,z)

D–H···A	D–H	H···A	D···A	D–H···A
N1–H1A···O3$^{(i)}$	0.85(3)	2.21(3)	3.045(3)	165
C7–H7···O3	1.02(3)	2.43(3)	2.804(3)	100.6(19)
C18–H18A···O2	0.96	2.48	2.823(4)	101
C19–H19C···O4	0.97	2.31	2.679(5)	102

3.3 Hirshfeld surface analysis

The intermolecular interactions of the crystal packing were studied through 3-D Hirshfeld surface and 2-dimensionl finger print representation with aid of crystal explorer 3.0 [42]. Besides their graphical visualization, it offers more relevant insight on chemical interactions and estimating the relative contribution of inter contacts. The HS surface plotted against the various properties such as de, dnorm, and curvedness has found to be an effective graphic tool for studying the molecular interactions and molecular crystal packing nature [43]. The interaction of the atoms depicted through various color including white, blue and red. The red color denoted as higher electron density, high H-bonding potentiality with closer contacts to the HS. The blue color denoted as the lower electron density with longer contacts and white region denoted as wander Waals separation [44]. The curvedness determined by curvature of HS. The low curvedness signifies the covalent bonding interactions and blue outline with large curvedness promulgates π - π interactions [45]. The H-bonding contact in the crystal is indicated as dark red color. Whereas, the H—H, C—H and C—Br interactions are appeared as light red color on the HS. The Hirshfeld surfaces (d_{norm}, Curvedness, Shape index) and finger pot representation is shown **Fig.6**. From d_{norm} surface diagram revealed that the dark red color shows the shorter interatomic contact with strong hydrogen bonding (N-H) of the 1,4 dihydro pyridine ring. The H—H contact appeared on middle of the surface with 55.5% contribution which is found to be higher compared to other intermolecular interactions. The O-H contact exhibited 15.0 % contribution to the Hirshfeld surface which is exhibited in the sharp spike. Moreover, C-H and Br-H interactions were found to be 12.1 % and 12.5 % respectively. The Br—C and N—H appeared as closer contact with

2.0% and 0.3 % to the Hirshfeld surfaces. The remaining inters contact interaction of the molecule with their percentage of contribution are shown **Fig. 7**.

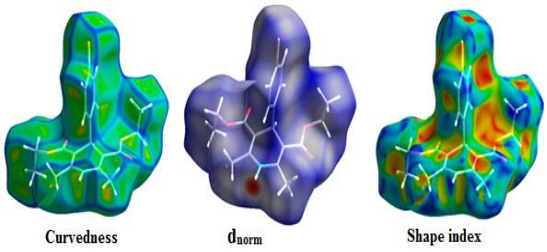

Fig.6. Hirshfeld Surfaces of the title compound

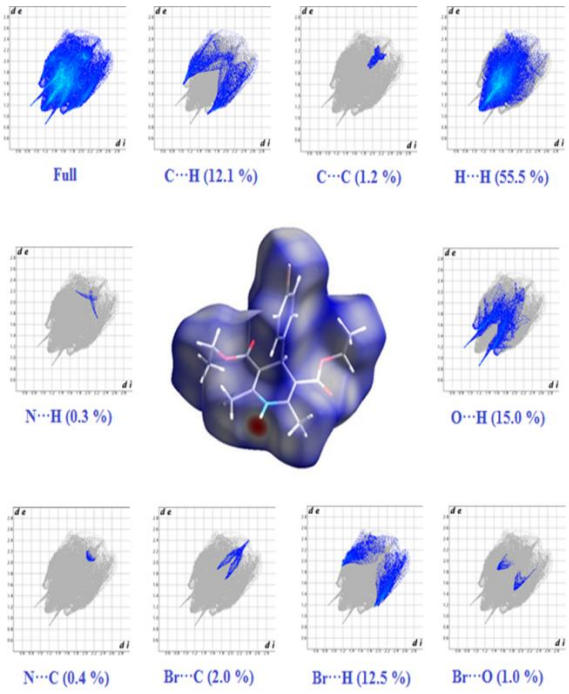

Fig.7. 2-D finger plot representaion of title compound showing individual contribution of each to the total Hirsheld surfaces.

3.4 Frontier Molecular Orbital energies analysis

The quantum mechanical calculation has been carried out by using DFT- Gaussian 09 version by B3LYP/6-311++G(d,p) method. The electronic behavior of the molecule is based the frontier molecular orbital energies. However, the highest occupied molecular orbital (HOMO) which carries electron with high energy and it has tendency to donate electron which is regarded as electron donor (nucleophile character). However, the lowest unoccupied molecular orbital (LUMO) with least energy tends to accept electron density which is denoted as an electron acceptor (electrophilic character) [46]. The energy gap within HOMO-LUMO was also used to describes the softness and hardness, molecular reactivity, kinetic stability, polarisability [47,48]. The chemical nature of the title compound was determined by HOMO and LUMO analysis. The DFT calculation is good correlation with experimental methods and their geometric comparison are given in **Table S1**. The calculated frontier molecular descriptors of crystal phase and DFT phase are given in **Table 5**. The molecular orbital energies were observed for the title compound (Crystal phase) are EHOMO= -5.82eV and ELOMO= -1.42. However, molecular orbital energies were observed for title compound (DFT phase) are EHOMO= -5.93Ev and ELOMO= -1.60. The DFT mapped surface of the compound is displayed in **Fig. 8.** In energy gap are found for Egap= 4.33eV (crystal phase) and E_{gap}= 4.32 eV (DFT phase). This energy gap of crystal phase and gas phase discloses that the molecule possess high chemical reactivity and low kinetic stability.

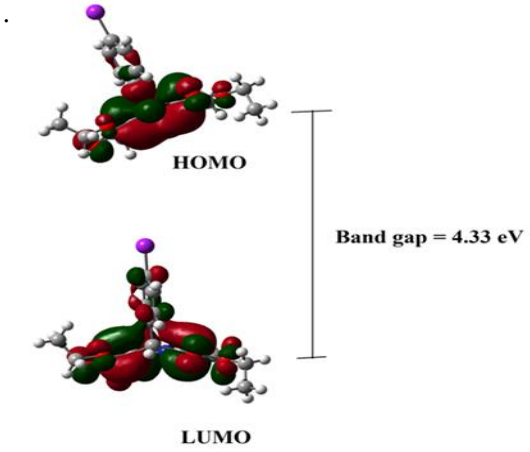

Fig.8. 3-Dimensional HOMO-LUMO surface

Table 5. Molecular descriptors of Crystal phase and DFT phase

Molecular descriptors	Crystal phase Energy (eV)	DFT phase
Electron affinity A= [-E_{LOMO}]	1.420707	1.601935
Ionization potential I= [-E_{HOMO}	5.820518	5.930997
Global hardness Ƞ=(I+A)/2	2.199906	2.164531
Electrochemical potential μ=-(I+A)/2	-3.62061	-3.76647
Electrophilicity	1.126088	1.195943

$\omega=\mu^2/2I$]		
Electronegativity $\chi=(I+A)/2$	3.620613	3.766466
HOMO energy	-5.820518	-5.930997
LUMO energy	-1.4207072	-1.6019351

3.3. Molecular Electrostatic potential analysis (MEP)

The molecular electrostatic potential (MEP) analysis has been carried out for the determination of hydrogen bonding interaction with assistance of electron density. However, 3-D MEP surface of the compound was visualized by different colors, in which electron-rich site appears at the red color, (most negative) and electron deficient-site appears at blue color (most positive). The yellow and light blue color indicates slightly electron deficient site [49, 50].

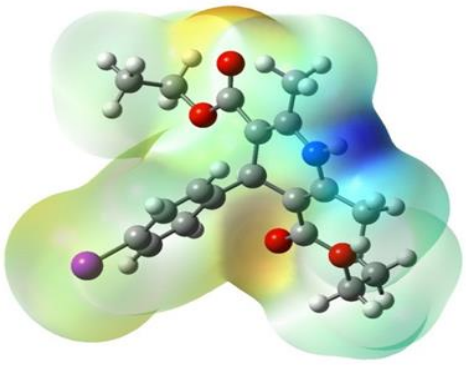

Fig 9. MEP surface of the molecule

Fig.7 describes the electronic nature of the molecule and oxygen atom is appeared electron rich site which possess negative charge with electrophilic character. The nucleophilic character was observed in blue color at N-H. The yellow and light blue color appears on the alkyl and benzene ring which indicate slightly electron deficient region which reveals the nucleophilic character.

4. Conclusion

In summary the crystallized compound 4-(4-Bromo-phenyl)-2,6-dimethyl-1,4-dihydro-pyridine-3,5-dicarboxylic acid diethyl ester has been developed by slow evaporation strategies utilizing ethanol as a solvent. Subsequently, the spectral methods such as FT-IR, ^{1}H NMR and ^{13}C NMR analysis has been used to determine the structure and functional group present in the molecule. Further the molecular structure was established through SC-XRD analysis and compound exhibit monoclinic with P21/n1 space group. The crystal and molecular structure is stagnated by N—H—O bonding. The Hirshfeld and 2D-finger plot representation reveals that H—H inter contacts are appeared the highest contribution 55.5 %. In addition the DFT analysis indicates that the crystallographic parameters are in well correlation with DFT parameters. The energy gap for the crystal is E_{gap}4.33eV which indicates that the compound possesses high chemical reactivity. Furthermore, the MEP analysis revealed that alkyl and benzene ring are in the most positive region which is more favorable for the nucleophilic character.

Acknowledgments

We record our sincere thanks to the (CIMF), Periyar University, Salem for providing the facilities for single crystal XRD analysis and SAIF-VIT for providing ^{1}H, ^{13}C NMR analysis. The author's also thanks to Jamal instrumentation facility (JIF), Post Graduate and Research Department of Chemistry, Jamal Mohamed College, Tiruchirappalli for providing necessary lab facilities.

References

[1] R.T. Morrison, R.N. Boyd, Organic Chemistry, 6th ed., Prentic-Hall of India, New Delhi, **2002.**

[2] A.R. Katritzky , C.A. Ramsden , J.A. Joule , V.V. Zhdankin , Handbook of Heterocyclic Chemistry, 3rd ed. *Elsevier*, Netherlands, **2010**.

[3] A. Hantzsch, Condensationsprodukte aus Aldehydammoniak und ketonartigen Verbindungen, *EurJIC.*, **1881**.

[4] D. J. Triggle, Calcium channel antagonists: clinical uses--past, present and future, *Biochem. Pharmacol.*, 74, **2007**, 1.

[5] F, Bossert, H Meyer and E. Wehinger, Angew, 4-Aryldihydropyridines, a New Class of Highly Active Calcium Antagonists, *Chemie Int. Ed. English.*, **1981**, 20, 762.

[6] S. Cosconati, L. Marinelli, A. Lavecchia, E. Novellino, Characterizing the 1,4-Dihydropyridines Binding Interactions in the L-Type Ca2+ Channel: Model Construction and Docking Calculations, *J. Med. Chem.*, **2007**, 50, 1504.

[7] Ilona Domracheva, Iveta Kanepe-Lapsa, Reinis Vilskersts, Imanta Bruvere, Egils Bisenieks,

Astrida Velena, Baiba Turovska, Gunars Duburs, . 4-Pyridinio-1,4-Dihydropyridines as Calcium Ion Transport Modulators: Antagonist, Agonist, and Dual Action, *Oxid Med Cell Longev*., **2020**, 20, 75815.

[8] F.H Siddiqi, Menzies, F.M. Lopez, A. E Stamatakou, C. Karabiyik, R. Ureshino, T . Ricketts, M.Jimenez-Sanchez, M.A.Esteban, L Lai,. Nat. Commun., **2019**, 10, 1718.

[9] Y. Zhang, J.Wang, Y. Li, F. Wang, F.Yang, W. Xu, Synthesis and Radioprotective Activity of Mitochondria Targeted Dihydropyridines in Vitro, Int. *J. Mol. Sci*., **2017**, 18, 2233.

[10] E. Leonova, K. Ošin, a, G. Duburs, E. Bisenieks, D. Germini, Y. Vassetzky, N. Sjakste, Metal ions modify DNA-protecting and mutagen-scavenging capacities of the AV-153 1,4-dihydropyridine, Mutat. Res. Genet. *Toxicol. Environ. Mutagen.*, **2019**, 845, 403077.

[11] D. Da Costa Cabrera, E. Santa-Helena, H.P. Leal, R.R. de Moura, L.E. M. Nery, C.A.N. Gonçalves, D. Russowsky, M.G. Montes D'Oca, Synthesis and antioxidant activity of new lipophilic dihydropyridines, *Bioorg. Chem*., **2019**, 84, 1–16.

[12] M. Sobhi Gomha, A. Zeinab Muhammad, M. Hassan, Abdel-aziz, K. Islam Matar & Abdelaziz A. El-Sayed, Green synthesis, molecular docking and anticancer activity of novel 1,4-dihydropyridine-3,5-Dicarbohydrazones under grind-stone chemistry, *Green Chemistry letters and Reviews*., **2020**, 13, 6–17.

[13] A. González, J. Casado, E.; Chueca, S. Salillas, A. Velázquez-Campoy, V.E. Angarica, L. Bénejat, J. Guignard, A. Giese, Repurposing dihydropyridines for treatment of helicobacter pylori infection, J. Sancho, *Pharmaceutics*., **2019,** 11681.

[14] S. Bahekar, D. Shinde, Synthesis and anti-inflammatory activity of 1, 4- dihydropyridines, *Acta pharmaceutica*., **2002**, 52, 281-287.

[15] B. Love, M. Goodman, K. Snader, R. Tedeschi, E. Macko, Hantzschtype dihydropyridine hypertensive agent, *J Med Chem*., **1974**, 17(9), 956-965.

[16] A.M. Vijesh, A.M. Isloor, S.K. Peethambar, K.N. Shivananda, T. Arulmoli, N.A.Isloor, Hantzsch reaction: synthesis and characterization of some new 1,4-dihydropyridine derivatives as potent antimicrobial andantioxidant agents, *Euro. J. Med. Chem*., **2011**, 46, 5591–5597.

[17] A. Debache, R. Boulcina, A. Belfaitah, S. Rhouati, B. Carboni, One-Pot Synthesis of 1,4-Dihydropyridines via a Phenylboronic Acid Catalyzed Hantzsch Three-Component Reaction, *Synlett.*, 2008, 509.

[18] S. Ko, M. N. V. Sastry, C. Lin, C. F. Yao, Synthesis of Hantsch 1,4-dihydropyridines by fermenting bakers! Yeast, *Tetrahedron Lett*., **2005**, 465-771.

[19] M . Litschauer, M. A. Neouze Nanoparticles, connected through an ionic liquid-like network, *J. Mater. Chem.* **2008** 18 640S.

[20] M.S. Souza, L.F. Diniz, N. Alvarez, C.C.P. da Silva, J. Ellena, Supramolecular synthesis and characterization of crystalline solids obtained from the reaction of 5-fluorocytosine with nitro compounds, *New J. Chem.* **2019**, 43, 15924–15934

[21] C. S. Chidan Kumar, K. Govindarasu, H. K. Fun, E. Kavitha, S. Chandraju, C. K. Quah, Synthesis, molecular structure, spectroscopic characterization and quantum calculation studies of (2E)-1-(5-chlorothiophen-2-yl)-3-(2,3,4-trimethoxyphenyl) prop-2-en-1-one, *J. Mol. Struct*. **2015**, 1085, 5 63-77

[22] Henrik F. Clausen, Marie S. Chevallier, Mark A. Spackman, and Bo B. Iversen, Three new co-crystals of hydroquinone: crystal structures and Hirshfeld surface analysis of intermolecular interactions‖, *New J. Chem*., **2010**, 34, 193–199

[23] Raouf Boulcina, Sofiane Bouacida, Thierry Roisnel, Abdelmadji Debache. Diethyl 4-(4-bromophenyl)-2,6-dimethyl-1,4-dihydropyridine-3,5-dicarboxylate, *Acta Crystallogr. Sect. E*., **2007**, E63, o3635–o3636

[24] R. Shashi, N.L. Prasad, N.S. Begum. One-Pot Synthesis of 1,4-Dihydropyridine Derivatives and Their X-Ray Crystal Structures: Role of Fluorine in Weak Interactions, J. Struct. Chem., **2020**, 61, 938-947

[25] D. Parthasarathi, M. Syed Ali Padusha, S. Suganya, P. Kumaradhas, Fares M Howari, Yousef Nazzal, Cijo Madathil Xavier, A. Meera Moydeen, Ayyiliath M. Sajith. Synthesis, Crystal structure, DFT calculations and Antimicrobial activity of 4-(4-Fluoro-phenyl)-2,6-dimethyl-1,4-dihydro-pyridine-3,5-dicarboxylic acid diethyl ester, *Egypt. J. Chem*. **2021** 64, 8, 4583 - 4590

[26] Bruker, APEX2, SAINT, and SADABS, 2006.
[27] G.M. Sheldrick, Crystal structure refinement with SHELXL, *Acta Crystallogr. Sect. C Struct. Chem.* **2015**, 71 3–8
[28] G.M. Sheldrick, A short history of SHELX, *Acta Crystallogr*., **2015**, A64 1, 112–122.
[29] G.M. Sheldrick, A short history of SHELX, Acta Crystallogr. Sect. A Found. *Crystallogr*., **2008**, 64, 112–122.
[30] C.F. Macrae, P.R. Edgington, P. McCabe, E. Pidcock, G.P. Shields, R. Taylor, M. Towler, J. Van De Streek, Mercury: visualization and analysis of crystal structures, J. Appl. Crystallogr., **2006** 39, 453–457.
[31] L.J. Farrugia, WinGX and ORTEP for Windows: an update, *J. Appl. Crystallogr*., **2012** 45, 849–854.
[32] Becke, A.D. Density-functional exchange-energy approximation with correct asymptotic behavior, Phys. Rev. A., **1998** 38, 3098.
[33] D. Hayakawa, N. Sawada, Y.Watanabe, H. Gouda, A molecular interaction field describing nonconventional intermolecular interactions and its application to protein–ligand interaction prediction, *J. Mol. Graph. Model*., **2020**, 96, 107515.
[34] Suresh Suganya, Ammasai Karthikeyan, Vadivel Srimathi, Poomani Kumaradhas, Supramolecular Co-crystal of 2-amino-4-methoxy-6-methyl pyrimidine with sorbic acid: Synthesis, crystal structure and Hirshfeld surface analysis, *Chem Data Collect.*, **2020**, 29, 100521.
[35] M. G. Sharma, D. P. Rajani, H. M. Patel, Green approach for synthesis of bioactive Hantzsch 1,4-dihydropyridine derivatives based on thiophene moiety via multicomponent reaction, R. Soc. open sci., **2017**, 41, 70006.
[36] Srinivas Nayak Amgoth, Mahendar Porika, Sadanandam Abbagani, Achaiah Garlapati, Malla, Reddy Vanga, Synthesis, anticancer and MRP1 inhibitory activities of 4-alkyl/aryl-3,5-bis(carboethoxy/carbomethoxy)-1,4-dihydro-2, 6-dimethylpyridines, *Med Chem Res*. 22 (2013)147–155.
[37] Akansha Agrwal, Virendra Kasana, [Fesipmim]Cl as highly efficient and reusable catalyst for solventless synthesis of dihydropyridine derivatives through Hantzsch reaction, *J. Chem. Sci*. **2020**, 132:67
[38] S. A. steiger, C. Linden, N.R. Natale, Crystal structure of ethyl 4-[4-(di-methyl-amino)-phen-yl]-2,7,7-trimethyl-5-oxo-1,4,5,6,7,8-hexa-hydro-quinoline-3-carboxyl-ate, Acta Cryst. **2018**. E74, 1417-1420
[39] A. Linden, R. Simsek, M. Gunduz, C. Safak, (±)-Methyl and (±)-ethyl 4-(2,3-di-fluoro-phen-yl)-2,6,6-trimethyl-5-oxo-1,4,5,6,7,8-hexa-hydro-quinoline-3 carboxyl-ate, *Acta Cryst.*, **2005**, C61, o731–o734.
[40] Wan-Sin Loh, Hoong-Kun Fun, B. Palakshi Reddy, V. Vijayakumar, S. Sarveswari, Dimethyl 1,4-dihydro-4-(4-methoxyphenyl)-2,6-dimethylpyridine-3,5- dicarboxylate, *Acta Cryst.* **2010**., E66, o587–o588
[41] Ming-Sheng Bai, Yan-Yun Chen, Dong-Ling Niu, Li Peng, Diethyl 2,6-dimethyl-4-phenyl-1,4-dihydropyridine-3,5-dicarboxylate, *Acta Cryst*. 2009, E65, o799
[42] P. Dhamodharan, K. Sathya, M. Dhandapani, Systematic evaluation of a new organic material:1-methyl-1H-imidazol-3-ium-2,4,6-trinitrobenzene-1,3-bis(olate)spectral, surface studies structural, electrical, optical, quantum chemical and Hirshfeld for optoelectronics through spectral, structural, electrical, optical, quantum chemical and Hirshfeld surface studies, *J. Phy. & Chem. Solids*., **2017**, 104, 175–184.
[43] K. Govindarasu, E. Kavitha, Molecular structure, Vibrational spectra, NBO, UV and first order Hyperpolarizability, analysis of 4-Chloro-DL-phenylalanine by Density Functional Theory‖, *Spectrochimica Acta Part A: Molecular and Biomolecular Spectroscopy*, **2014**, 133, 10 799-810,
[44] Kaliyaperumal Thanigaimani, Nuridayanti Che Khalib, Ersin Temel, Suhana Arshad, Ibrahim Abdul Razak, New supramolecular cocrystal of 2-amino-5-chloropyridine with 3- methylbenzoic acids: Syntheses, structural characterization, Hirshfeld surfaces and quantum chemical investigations, *J. Mol. Struct*., **2015**, 1099, 246-256.
[45] R. Shobha Prabhu, A. Jayarama, K. Chandrasekharan, V. Upadhyaya, Seik Weng Ng, Synthesis, growth, structural characterization, Hirshfeld analysis and nonlinear optical studies of a methyl substituted chalcone, *J. Mol. Struct*., **2017** 1136, 244e252.
[46] M.A. Spackman, J.J. McKinnon, Crystalline packing in pentacene-like organic semiconductors, *CrystEngComm*., **2002**, 4, 378–392.

[47] C. Kalaiarasi, P. Sangeetha, M.S. Pavan, P. Kumaradhas, Crystal structure and theoretical charge density studies of dilantin molecule, *J. Mol. Struct.*, **2018**, 1170, 105–118

[48] M. Raja, R. Raj Muhamed, S. Muthu, M. Suresh. Synthesis, spectroscopic (FT-IR, FT-Raman, NMR, UV–Visible), NLO, NBO, HOMO-LUMO, Fukui function and molecular docking study of (E)-1-(5-bromo-2-hydroxybenzylidene) semicarbazide, *J. Mol. Struct*., 2017, 1141, 284-298.

[49] Rajesh Kumar, Amit Kumar, Vipin Deval, Archana Gupta, Poonam Tandon, P. S. Patil, Prathmesh Deshmukh, Deepika Chaturvedi, J. G. Watve. Molecular structure, spectroscopic (FT-IR, FT Raman, UV, NMR and THz) investigation and hyperpolarizability studies of 3-(2-Chloro-6-fluorophenyl)-1-(2-thienyl) prop-2-en-1- one, *J. Mol. Struct*., **2017**, 1129, 292-304.

[50] M. Raja, R. Raj Muhamed, S. Muthu, M. Suresh. Synthesis, spectroscopic (FT-IR, FT-Raman, NMR, UV–Visible), NLO, NBO, HOMO-LUMO, Fukui function and molecular docking study of (E)-1-(5-bromo-2-hydroxybenzylidene)semicarbazide, *J. Mol. Struct.*, **2017**, 5, 284-298.